Separation Science and Technology
Publication details, including instructions for authors and subscription information:
http://www.informaworld.com/smpp/title~content=t713708471

Perturbations of the Retention Parameter Due to Sample Overloading in Hollow-Fiber Flow Field-Flow Fractionation

Alf Carlshaf[a]; Jan Åke Jönsson[a]
[a] DEPARTMENT OF ANALYTICAL CHEMISTRY, UNIVERSITY OF LUND, LUND, SWEDEN

To cite this Article Carlshaf, Alf and Jönsson, Jan Åke(1993) 'Perturbations of the Retention Parameter Due to Sample Overloading in Hollow-Fiber Flow Field-Flow Fractionation', Separation Science and Technology, 28: 5, 1191 — 1201
To link to this Article: DOI: 10.1080/01496399308018029
URL: http://dx.doi.org/10.1080/01496399308018029

SEPARATION SCIENCE AND TECHNOLOGY, **28**(5), pp. 1191–1201, 1993

Perturbations of the Retention Parameter Due to Sample Overloading in Hollow-Fiber Flow Field-Flow Fractionation

ALF CARLSHAF and JAN ÅKE JÖNSSON*
DEPARTMENT OF ANALYTICAL CHEMISTRY
UNIVERSITY OF LUND
P.O. BOX 124, S-22100 LUND, SWEDEN

Abstract

We report on the perturbations on the retention parameter in hollow-fiber flow field-flow fractionation that is caused by sample overloading. The overloading phenomenon is connected to the sample concentration at the channel wall, and an equation for calculating this concentration is presented. It is shown that the expression can be used to approximate the maximum amount of sample that can be loaded and how it depends on the fiber radius. The loadability dependence on the ionic and field strength is also investigated.

INTRODUCTION

Flow field-flow fractionation (flow-FFF) is a subtechnique in the general group of separation methods for macromolecules and particles named field flow fractionation (*1*, *2*). All methods in the group utilize a flow of liquid through a separation channel as a carrier for the solute and a perpendicularly applied force field to cause a lateral migration of the solute toward one of the channel walls. In flow-FFF, this lateral migration is caused by a secondary flow, directed transverse to the elution flow. Close to the wall, the sample cloud will equilibrate into an exponential concentration distribution, forming a zone with a specific average thickness. The thickness of the zone (which depends on the magnitude of the force field and/or the properties of the sample) will determine its axial velocity through the

*To whom correspondence should be addressed.

channel by its mean lateral position in the parabolic flow profile that is developed under laminar flow conditions. The concept was first developed by J. C. Giddings (*3*).

In previous papers (*4*, *5*) we presented an alternative way of performing flow-FFF by using a cylindrical hollow fiber as a separation channel instead of the classical parallel plate configuration (*6*, *7*). The cylindrical geometry of the separation channel and the instrumental setup for this version of flow-FFF, with independent and precise control of the two flows (axial and radial), simplifies the operation.

The theoretical basis of hollow-fiber flow-FFF is sufficiently rigorous to allow the calculation of the diffusion coefficient, and thus the Stokes diameter of the particles, for uncharacterized molecules and colloidal particles based on experimentally measured retention parameters. The efficiency, however, does not agree as well with theory. The main reason for this was shown to be the inhomogeneous pore distribution in the fiber wall, which gives an additional band-broadening effect (*8*). The inhomogeneous porosity will not affect the retention time which is dependent only on the overall total radial flow.

To improve the accuracy of retention measurements, several experimental parameters must be controlled. It has been shown that the ionic strength of the elution medium is a crucial parameter that must be adjusted in order to minimize the interaction forces between the particles and, especially, between the particles and the wall to prevent adsorption (*9–12*). The pH and temperature are other parameters that affect the fractionation results (*13*) by altering the surface properties of both the sample and the channel wall. The diffusion coefficient and the viscosity of the elution medium are also affected by the temperature. If a detergent is used to prevent aggregation of particles, the type of surfactant could have an influence on the results (*14*) by the way it adheres to the surfaces and alters their properties.

Another important parameter that affects the elution behavior is sample load (*11*, *13*, *15*). Too high a concentration of particles in the sample zone will lead to increased particle–particle interactions so the particles can no longer be approximated as "noninteracting point particles," which is assumed by theory. It also increases the viscosity (*16*) near the wall, decreasing the diffusion coefficient, which leads to an increased retention time. The change in viscosity will additionally disturb the laminar flow near the wall, and the expected parabolic flow profile will not be established.

The effects of overloading lead to deviation from ideal behavior (i.e., elution under ideal conditions without additional forces acting on the particles except the radial flow and a perfect axial parabolic flow profile). The sample zone can reach the "overcrowded" state without large amounts of sample being injected if the separation conditions are badly chosen.

For this paper we investigated the departures from ideality by injecting different concentrations of polystyrene latex beads at different field and ionic strengths.

EXPERIMENTAL

The hollow-fiber flow-FFF system has been described in detail earlier (*4*). Briefly, the apparatus is based on the FPLC range of liquid chromatographic equipment (Pharmacia LKB, Uppsala, Sweden). The hollow fiber used in all the experiments was of model Harp HF1.0-43-PM100 and made of polysulfone (Supelco, Inc., Bellefonte, Pennsylvania, USA; produced by Romicon, Inc., Woburn, Massachusetts, USA). The inner diameter and length was 1100 μm and 24 cm, respectively. The fiber was encapsulated in an empty, modified glass column intended for low-pressure chromatography (Model C 10/20, Pharmacia LKB). Sample was injected with an internal volume injection valve (Model 7410, Rheodyne Inc., Cotati, California, USA) equipped with a pneumatic actuator unit. The injection volume was 5 μL in all experiments. Detection was by a fixed wavelength (254 nm) UV detector (UV-1, Pharmacia LKB). The axial and radial flows were created by three syringe pumps (model P-500, Pharmacia LKB) connected to the fiber. The pumps were further connected to a computerized control unit (LCC-500, Pharmacia LKB) which was programmed to control the flow and composition of eluent (by mixing flows from two of the pumps) in the axial direction and the radial flow independently as well as the injection valve.

Polymer latex particles (Sigma, St. Louis, Missouri, USA) with a diameter of 0.091 μm (SD = 0.0058 μm) were used in all the experiments. They were diluted with eluent (water solution of 0.1% Triton X-100 and varying concentrations of NaCl) to six different concentrations (20, 10, 2, 1, 0.4, and 0.2 mg/mL). The suspensions with polystyrene particles were sonicated for about 1 hour before use to disrupt particle aggregates. The water used was purified with a Milli-Q/RO-4 unit (Millipore, Bedford, Massachusetts, USA).

THEORY

For the derivation of an equation that relates retention time to the size distribution for an unknown sample, it is crucial that there are no interparticle interactions and also no interactions between the particles and the wall. This is impossible to accomplish completely, but it is possible to minimize these interactions by adjusting the ionic strength and by not overloading the separation channel. The sample zone has its highest concentration at the beginning of the elution process, before it becomes diluted by different band-broadening mechanisms (*8*). The particle concentration within the zone has its maximum in the center of the zone and closest to

the wall (*15*). The number of particles decreases exponentially in the radial direction. In the axial direction they decrease according to the Gaussian distribution when moving away from the center of the zone.

The maximum concentration must be kept below a certain critical concentration (C_{crit}) by injecting small sample masses and by keeping the radial flow as low as possible in order to minimize particle–particle interactions and premature elution.

The maximum concentration of particles depends on several factors:

(a) The ionic strength of the elution media
(b) The injected mass
(c) The diffusion coefficient of the particles
(d) The field strength (radial flow)

The theoretical treatment of hollow-fiber flow-FFF is described in detail elsewhere (*4*), and here we will give only the equations necessary for calculating the sample concentrations close to the wall at different experimental conditions. The concentration at the wall can be calculated by using the expression for the radial distribution of sample in the fiber:

$$C = C_0 \exp\left(\mathrm{Pe}\left((r/R)^2 - \frac{(r/R)^4}{4}\right)\right) \tag{1}$$

The Peclet number (Pe) is defined as

$$\mathrm{Pe} = U_R \frac{R}{D} \tag{2}$$

where r is the radial coordinate, U_R is the radial (linear) flow at the wall ($U_R = F_R/2\pi RL$), F_R is the volumetric radial flow, L is the fiber length, R is the fiber radius, D is the diffusion coefficient of the sample particles, and C_0 is the particle concentration in the center of the fiber. If the injected sample plug is assumed to occupy the same volume in the fiber as the injection volume v_{inj}, the mean concentration of sample $\langle C \rangle$ will be

$$\langle C \rangle = \frac{m_{inj}}{v_{inj}} \tag{3}$$

where m_{inj} is the injected mass.

The mean concentration can also be derived from Eq. (1) by calculating the average of the function, giving

$$\langle C \rangle = C_0 \frac{\sqrt{\pi}}{\sqrt{\mathrm{Pe}}} \exp\left((\mathrm{Pe})\left(\operatorname{erf}\sqrt{\mathrm{Pe}} - \operatorname{erf}\frac{\sqrt{\mathrm{Pe}}}{2}\right)\right) \tag{4}$$

Combining Eqs. (3) and (4) gives an expression for C_0 that can be substituted into Eq. (1) to give the following expression for the concentration C_w at the wall, where $r = R$.

$$C_w = \frac{m_{inj}}{v_{inj}} \frac{\sqrt{\mathrm{Pe}}}{\sqrt{\pi}} \frac{\exp\left(-\frac{\mathrm{Pe}}{4}\right)}{\left(\operatorname{erf}\sqrt{\mathrm{Pe}} - \operatorname{erf}\frac{\sqrt{\mathrm{Pe}}}{2}\right)} \tag{5}$$

When plotting the wall concentration (C_w) against the injected mass (m_{inj}) by using Eq. (5) (Fig. 1), with a constant injection volume, v_{inj}, it can be seen that if the injected mass exceed a certain value, the wall concentration will theoretically increase above the concentration that corresponds to a face-centered cubic lattice of the particles C_{cp} (the dotted line in Fig. 1).

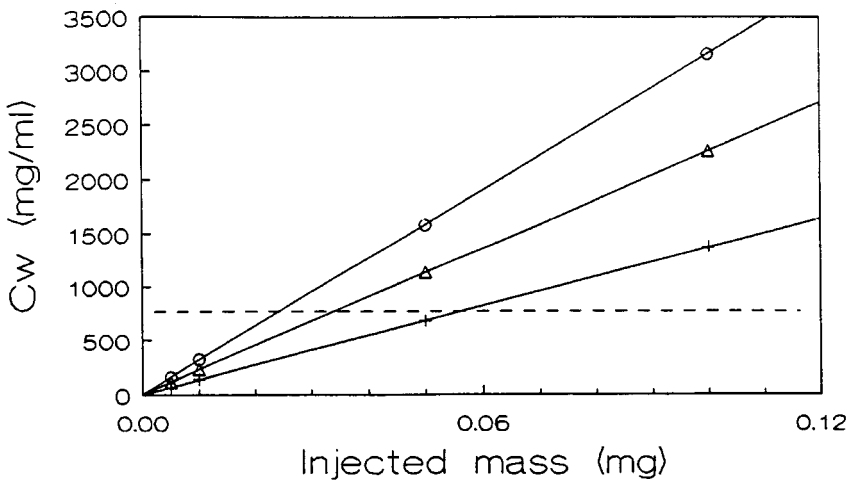

FIG. 1. Calculated wall concentration C_w (Eq. 5) plotted against the injected mass m_{inj} at three different radial flows. Injection volume is 5 μL. The masses marked in the plot are the four most concentrated samples that were injected in the experiments. (○) F_R = 0.14 mL/min, (△) F_R = 0.10 mL/min, (+) F_R = 0.06 mL/min.

Close packing of the particles is only possible when there are no repulsive interactions between the particles. At high ionic strength, the decrease in double-layer thickness will make it possible for the particles to pack very close together, and disturbances in the elution will occur at a different value of m_{inj} than they would with a lower ionic strength. Consequently, the value of C_{crit} will be dependent on the ionic strength. It will also be lower in practice than the concentration that corresponds to the close packing arrangement of the particles, C_{cp}, because the particles start to interact well before they are packed into a close-packed lattice.

One way to increase the loadability is to increase the radius of the fiber. Figure 2 illustrates the relationship between injected sample mass and that Peclet number which causes the injected sample to reach C_{crit} at the wall for two different radii (0.055 and 0.11 cm). Equation (5) was used with a fixed value on C_{crit} equal to 500 mg/mL instead of 740 mg/mL (C_{cp}). The length of the sample plug in the fibers is constant in the two cases, meaning that the fiber surface area against which the sample concentrates increases by a factor of 2 when the radius is doubled. The figure shows that the loadability increases by a factor of 2 [keeping the linear radial flow constant,

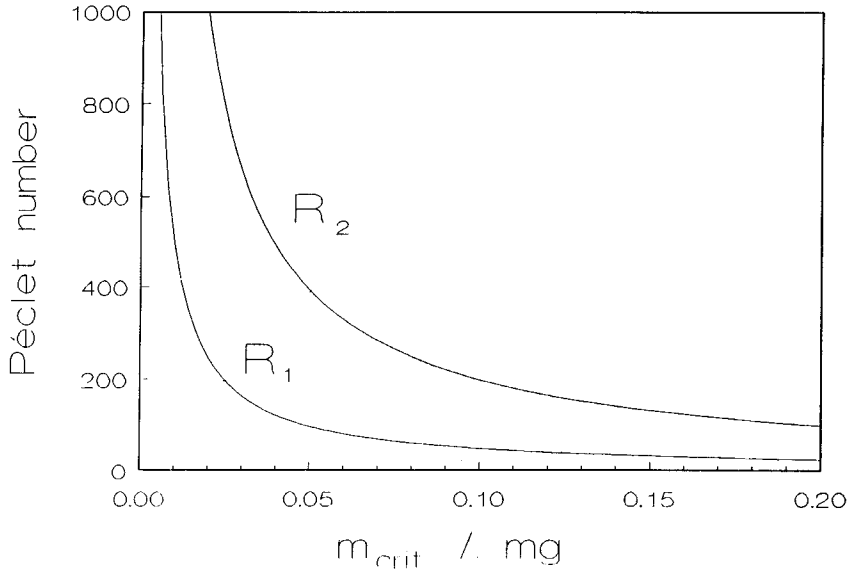

FIG. 2. Peclet number versus critical injected mass (m_{crit}). The curves shows the maximum mass that can be injected at different Peclet numbers for two different fiber radii (R_1 = 0.055 cm and R_2 = 0.11 cm). C_{crit} is set to 500 mg/mL, and v_{inj} is 5 and 20 μL, respectively.

i.e., an increase of the Peclet number by a factor of 2 (Eq. 2)] when the fiber radius is doubled. With a certain fiber radius, the loadability will decrease if a high separation efficiency is attempted by utilizing a high radial flow (i.e., a high Peclet number, see Fig. 2).

RESULTS AND DISCUSSION

The total injected mass of sample is directly connected to the particle concentration at the wall. If the injected amount of sample exceeds the critical mass m_{crit}, the particles at the wall will pack as closely as possible, approaching cubic close packing (the possibility of reaching this particle configuration increases with the ionic strength). This will lead to an increase in the mean particle layer thickness (with a decrease in elution time as a consequence) and to a drastic increase in viscosity (with the opposing effect on the elution time).

In Fig. 3 the ionic strength (I) of the elution medium is adjusted to minimize the interaction forces between particles and between particles and the wall, as described in Ref. *10* (to 1.75 mM). The concentration of polystyrene particles is varied between 0.2 and 20 mg/mL to give samples

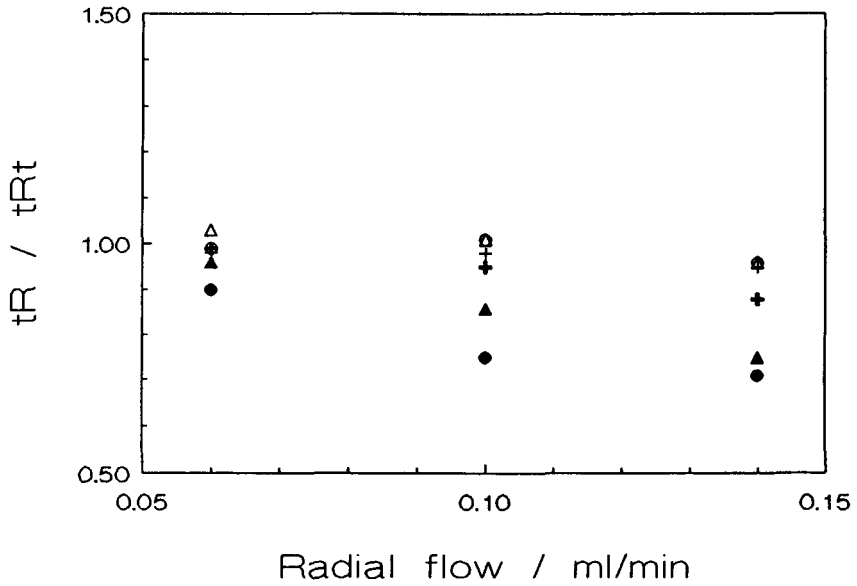

FIG. 3. Influence of sample concentration on the relative retention time. I = 1.75 mM (water with 0.1% Triton X-100 and NaCl). The axial flow was 0.6 mL/min in all cases. (●) 20 mg/mL, (▲) 10 mg/mL, (+) 2 mg/mL, (○) 1 mg/mL, (△) 0.4 mg/mL, (+) 0.2 mg/mL.

of six different concentrations. Each sample is injected at three different radial flows (F_r). The deviation from the theoretically expected retention time (t_{Rt}), calculated with Eq. (22) in Ref. *4*, t_R/t_{Rt}, is plotted against the radial flow. The figure shows that good agreement between experimental and theoretically expected retention times was obtained for the three lowest concentrations at all crossflows. A decrease in retention time was noticed at higher concentrations. The decrease became more pronounced as the concentration and crossflow were increased. This result agrees well with the theory presented above. Note that the wall concentration (Fig. 1) is close to or above the close packing concentration at all crossflows for the two most concentrated samples.

Figure 4 shows the same experiment at a lower ionic strength (1.0 mM). If I is too low, the electrical double layer will be extended and particles will repel each other to a greater extent. The consequence will be an expanded sample zone that may also be pushed away from the wall (if the channel wall has the same surface charge as the particles). The overloading tendencies appear at lower particle concentrations, and even at the lowest concentration a decrease in retention time was observed at the highest crossflow.

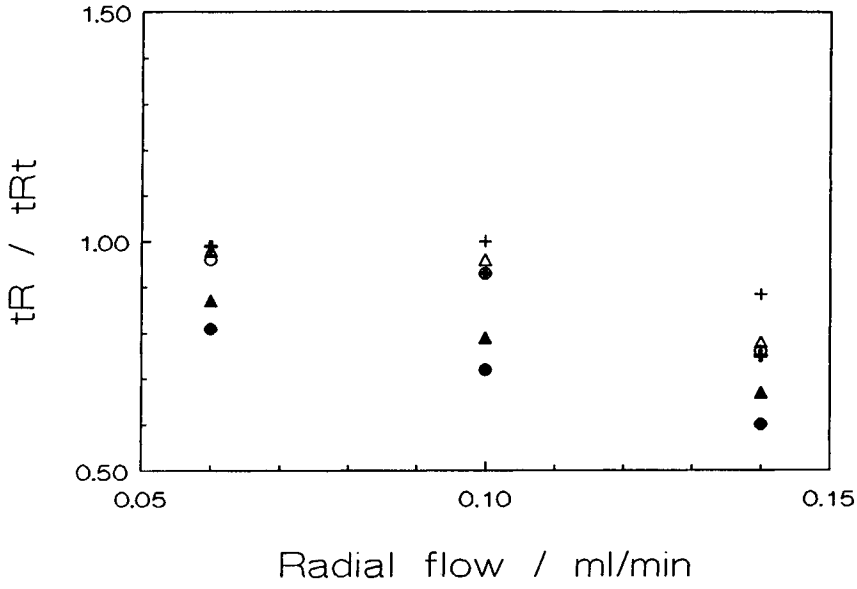

FIG. 4. As in Fig. 3, except I = 1.0 mM.

If the ionic strength is increased above 1.75 mM, there will be different opposing effects on the retention time, and the results become more unpredictable. The particles will be able to pack very closely because of the decrease in double-layer thickness, and the risk of particle aggregation will increase. The increased possibility of a close packing arrangement of the particles at high crossflows and/or high sample loads will increase the risk of disturbances in the parabolic flow profile near the wall as a consequence of increased viscosity. A very high particle concentration at the wall will cause a drastic increase in viscosity (*16*) and thereby a decrease of the diffusion coefficient, which will lead to increased elution time. Additionally, the attractive forces between the solute and the channel wall will be more pronounced at higher ionic strength, leading to prolonged elution times (*10*). These effects on the elution time are opposed by the increased mean thickness of the sample zone that will cause a decrease in elution time.

In Fig. 5 the experiment is repeated at an ionic strength of 2.0 mM. The lowest concentration (0.2 mg/mL) seems to be low enough to avoid particle–particle interaction and to avoid an increase in the mean thickness of the particle zone. The retention time for this concentration agrees well with theory at all crossflows. At the lowest crossflow (0.06 mL/min) there

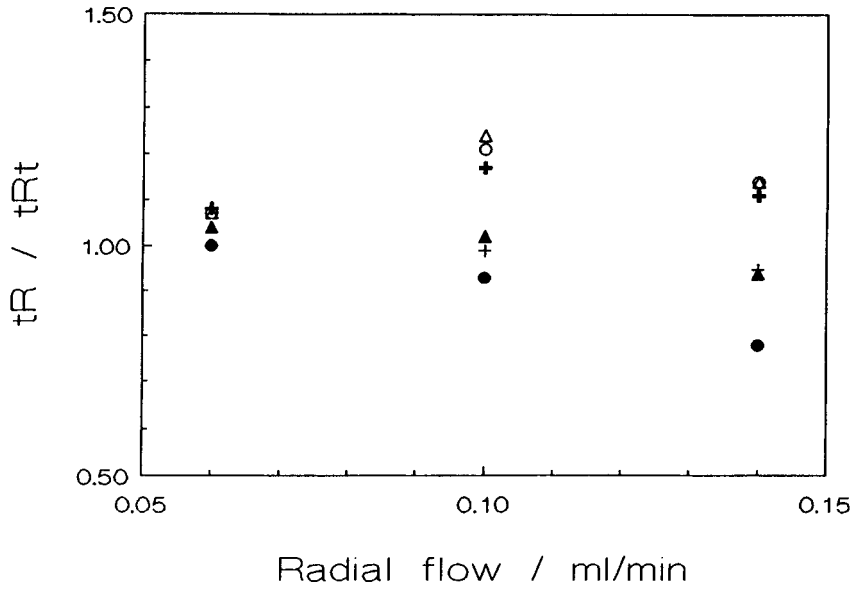

FIG. 5. As in Fig. 3, except I = 2.0 mM.

were no severe deviations from the theoretical retention time at any concentration. When the crossflow was increased to 0.10 mL/min, the lower concentrations (0.4, 1.0, and 2.0 mg/mL) showed an increase in retention time, probably due to the increased attractive interaction and/or an increase in viscosity near the wall. The most likely reason why the higher concentrations (10 and 20 mg/mL) did not show the same increase is that the viscosity and interaction effects were balanced by the opposing effect from the increase in mean layer thickness. The highest concentration (20 mg/mL) showed a slight decrease in retention caused by the increase in mean layer thickness. This tendency was amplified at the highest crossflow (0.14 mL/min). The explanation for this behavior must be that if the wall concentration becomes too high (at a high ionic strength), the effect of the increased mean layer thickness will dominate over the viscosity and attractive interaction effects. The fact that the retention time obtained for the most concentrated sample (20 mg/mL) was longer (at a crossflow of 0.14 mL/min) at an ionic strength of 2.0 mM than at 1.75 mM supports this conclusion (Figs. 3 and 5).

The derived expression (Eq. 5) can be used to estimate the maximum mass of an unknown sample that can be loaded onto a fiber (at a certain linear radial flow) of radius R without getting any disturbances on the retention parameter. Before making the approximation, C_{crit} must be found experimentally.

If the radius is changed from R_1 to R_2, the loadability will change with a factor equal to R_2/R_1 (while holding the linear radial flow constant), provided that the injection volume is changed accordingly with a factor of $(R_2/R_1)^2$.

Figure 2 shows, for example, that if the radial flow is set to achieve a Peclet number of 200 on a small fiber, the maximum mass of polystyrene particles that can be loaded is approximately 25 μg. If the radius is doubled (while holding the linear radial flow constant), the Peclet number will also be doubled (Eq. 2). The result will be a more efficient fractionation but at the cost of a longer retention time (the efficiency per unit of time, however, will decrease). Additionally, m_{crit} will increase to about 50 μg.

From a preparative point of view, this means that it is possible in a simple way to calculate the fiber radius necessary to fractionate a certain amount of sample.

Acknowledgment

This work was supported by the Swedish Natural Science Research Council.

REFERENCES

1. K. D. Caldwell, *Anal. Chem., 60,* 959A (1988).
2. J. Janca, *Field-Flow Fractionation: Analysis of Macromolecules and Particles,* Dekker, New York, 1988.
3. J. C. Giddings, *Sep. Sci., 1,* 123 (1966).
4. J. Å. Jönsson and A. Carlshaf, *Anal. Chem., 61,* 11 (1989).
5. A. Carlshaf and J. Å. Jönsson, *J. Chromatogr., 461,* 89 (1989).
6. K. G. Wahlund and J. C. Giddings, *Anal. Chem., 59,* 1332 (1987).
7. K. G. Wahlund, S. Winegarner, K. D. Caldwell, and J. C. Giddings, *Ibid., 58* (1986).
8. A. Carlshaf and J. Å Jönsson, *Sep. Sci. Technol., 28,* 1031 (1993).
9. Y. Mori, K. Kimura, and M. Tanigaki, *Anal. Chem., 62,* 2668 (1990).
10. A. Carlshaf and J. Å Jönsson, *J. Microcol. Sep., 3,* 411 (1991).
11. M. E. Hansen, J. C. Giddings, and R. Beckett, *J. Colloid Interface Sci., 132,* 300 (1989).
12. M. E. Hansen and J. C. Giddings, *Anal. Chem., 61,* 811 (1989).
13. A. Litzén and K. G. Wahlund, *J. Chromatogr., 548,* 393 (1991).
14. Y. Mori, B. Scarlett, and H. G. Merkus, *Ibid., 515,* 27 (1990).
15. K. D. Caldwell, S. L. Brimhall, Y. Gau, and J. C. Giddings, *J. Appl. Polym. Sci., 36,* 703 (1988).
16. I. M. Krieger, *Adv. Colloid Interface Sci., 3,* 111 (1972).

Received by editor December 2, 1991
Revised May 26, 1992